HHS Public Access

Author manuscript

Cell Rep. Author manuscript; available in PMC 2020 September 28.

Published in final edited form as:

Cell Rep. 2020 September 01; 32(9): 108087. doi:10.1016/j.celrep.2020.108087.

Lactate Dehydrogenase A Governs Cardiac Hypertrophic Growth in Response to Hemodynamic Stress

Chongshan Dai[1], **Qinfeng Li**[1,2,3], **Herman I. May**[1], **Chao Li**[1], **Guangyu Zhang**[1], **Gaurav Sharma**[4], **A. Dean Sherry**[4,5,6], **Craig R. Malloy**[4,5,7], **Chalermchai Khemtong**[4,5], **Yuannyu Zhang**[8,9], **Yingfeng Deng**[10], **Thomas G. Gillette**[1], **Jian Xu**[8,9], **David T. Scadden**[11,12,13], **Zhao V. Wang**[1,14,*]

[1]Division of Cardiology, Department of Internal Medicine, University of Texas Southwestern Medical Center, Dallas, TX 75390, USA

[2]Key Laboratory of Cardiovascular Intervention and Regenerative Medicine of Zhejiang Province, Hangzhou, Zhejiang 310016, China

[3]Department of Cardiology, Sir Run Run Shaw Hospital, School of Medicine, Zhejiang University, Hangzhou, Zhejiang 310016, China

[4]Advanced Imaging Research Center, University of Texas Southwestern Medical Center, Dallas, TX 75390, USA

[5]Department of Radiology, University of Texas Southwestern Medical Center, Dallas, TX 75390, USA

[6]Department of Chemistry, University of Texas in Dallas, Dallas, TX 75080, USA

[7]Department of Internal Medicine, University of Texas Southwestern Medical Center, Dallas, TX 75390, USA

[8]Children's Medical Center Research Institute, University of Texas Southwestern Medical Center, Dallas, TX 75390, USA

[9]Department of Pediatrics, Harold C. Simmons Comprehensive Cancer Center, and Hamon Center for Regenerative Science and Medicine, University of Texas Southwestern Medical Center, Dallas, TX 75390, USA

[10]Touchstone Diabetes Center, Department of Internal Medicine, University of Texas Southwestern Medical Center, Dallas, TX 75390, USA

*Correspondence: zhao.wang@utsouthwestern.edu.

AUTHOR CONTRIBUTIONS

C.D. and Z.V.W. conceived and designed the study. C.D. performed most experiments with help from Q.L., H.I.M., and G.Z. (animal surgery); G.S., A.D.S., C.R.M., and C.K. (metabolic analysis); and Y.Z. and J.X. (RNA-seq analysis). C.D. and Z.V.W. wrote the manuscript with the help of C.L., Y.D., T.G.G., and D.T.S. All authors revised and approved the manuscript.

DECLARATION OF INTERESTS

The authors declare no competing interests.

SUPPLEMENTAL INFORMATION

Supplemental Information can be found online at https://doi.org/10.1016/j.celrep.2020.108087.

[11]Department of Stem Cell and Regenerative Biology, Harvard University, Cambridge, MA 02138, USA

[12]Harvard Stem Cell Institute, Cambridge, MA 02138, USA

[13]Center for Regenerative Medicine, Massachusetts General Hospital, Boston, MA 02138, USA

[14]Lead Contact

SUMMARY

The heart manifests hypertrophic growth in response to high blood pressure, which may decompensate and progress to heart failure under persistent stress. Metabolic remodeling is an early event in this process. However, its role remains to be fully characterized. Here, we show that lactate dehydrogenase A (LDHA), a critical glycolytic enzyme, is elevated in the heart in response to hemodynamic stress. Cardiomyocyte-restricted deletion of LDHA leads to defective cardiac hypertrophic growth and heart failure by pressure overload. Silencing of LDHA in cultured cardiomyocytes suppresses cell growth from pro-hypertrophic stimulation *in vitro,* while overexpression of LDHA is sufficient to drive cardiomyocyte growth. Furthermore, we find that lactate is capable of rescuing the growth defect from LDHA knockdown. Mechanistically, lactate stabilizes NDRG3 (N-myc downregulated gene family 3) and stimulates ERK (extracellular signal-regulated kinase). Our results together suggest that the LDHA/NDRG3 axis may play a critical role in adaptive cardiomyocyte growth in response to hemodynamic stress.

In Brief

Dai et al. find that LDHA is significantly increased in the heart under hemodynamic stress, and cardiomyocyte-specific deletion of LDHA leads to severe cardiac dysfunction in response to pressure overload. LDHA may govern adaptive growth through elevation of NDRG3 and activation of ERK.

Graphical Abstract

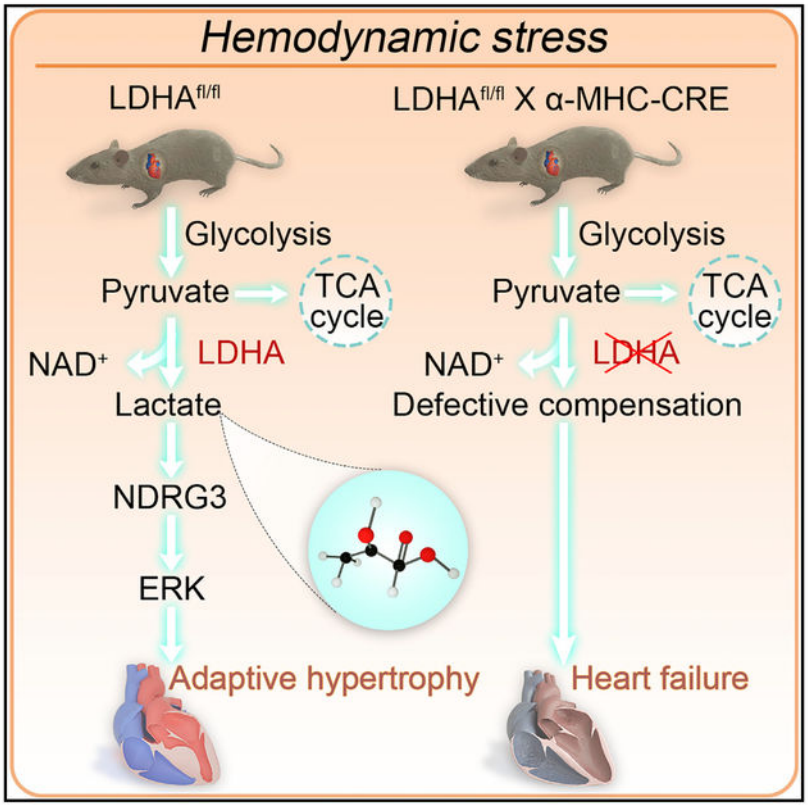

INTRODUCTION

Heart failure (HF) is a leading cause of death worldwide. With a 5year survival rate of approximately 50%, HF poses a major burden on the socioeconomic and healthcare systems (Benjamin et al., 2019). Despite the urgent and utmost clinical needs, our understanding of HF remains incomplete, and effective cures are missing.

Development of effective therapeutic intervention requires a better, more thorough understanding of the mechanism mediating the pathophysiology of HF. Hypertension is one of the most important risk factors of HF (Benjamin et al., 2019). In response to high blood pressure, the heart manifests significant growth to ameliorate ventricular wall stress and ensure effective pumping function. Because of limited regenerative capacity, cardiac growth is largely realized by an increase in individual cardiomyocytes. This concentric growth of the heart, once adaptive, may decompensate under persistent hemodynamic stress (Drazner, 2011). Past decades have witnessed extensive interest and tremendous progress in our understanding of this clinically relevant disease (Heineke and Molkentin, 2006; Nakamura and Sadoshima, 2018). However, the underlying mechanisms of cardiac growth and the transition from hypertrophy to HF are incompletely defined.

Pathological cardiac growth under pressure overload involves a spectrum of remodeling at various levels, including structural, electrophysiological, metabolic, and functional events (Hill and Olson, 2008). Studies have shown that metabolic alterations precede most if not all

of these processes, highlighting a possible causative role (Gibb and Hill, 2018; Ritterhoff and Tian, 2017; Sen et al., 2013; Tran and Wang, 2019). A healthy adult heart is an omnivore, consuming any nutrients available. While the majority of ATP production relies on combustion of free fatty acids, glucose and lactate oxidation also significantly contribute to the overall energy homeostasis (Kolwicz et al., 2013; Lopaschuk et al., 2010). During cardiac hypertrophic growth, the contribution from glucose and lactate is augmented from 30% to approximately half. This feature largely resembles cardiac metabolism during fetal development, which is driven by a return to the fetal gene program (Bertero and Maack, 2018; Taegtmeyer et al., 2010). Indeed, signaling molecules and enzymes of fatty acid β-oxidation are decreased, while pathways for glucose utilization are elevated during hypertrophic growth in the heart (Leong et al., 2003). However, it remains to be established whether this metabolic remodeling is adaptive to ensure the cardiac pumping function.

Glycolysis is a major route to catabolize glucose in a cell (Depre et al., 1999). A series of enzymatic reactions catalyze the conversion from glucose to lactate, and the latter is either excreted or oxidized. Previous studies have shown that glucose uptake is strongly upregulated from 2,400 to 3,600 nmol/g tissue weight in hypertrophic hearts compared to controls (Allard et al., 1994). Importantly, glucose oxidation (i.e., from pyruvate to ATP and CO_2 production) is not proportionally increased. This uncoupling between glycolysis and glucose oxidation raises an important question regarding the relevance of lactate production by lactate dehydrogenase A (LDHA), which may play other pivotal roles in addition to being a glycolytic product (Gladden, 2004). Indeed, recent studies suggest that lactate may act as a signaling molecule in controlling the differentiation of vascular smooth muscle cells (Yang et al., 2017) and maintaining the viability of cancer cells under hypoxia (Lee et al., 2015). These findings prompted us to investigate the role of LDHA and lactate in cardiac hypertrophic growth and HF under pressure overload.

RESULTS

LDHA Is Induced in the Heart by Hypertrophic Growth

To examine the relevance and mechanism of action of metabolic remodeling in cardiac hypertrophic growth, we conducted an unbiased RNA sequencing (RNA-seq) analysis (Figure 1A). We isolated neonatal rat ventricular myocytes (NRVMs) from 1- to 2-day-old Sprague-Dawley rats and cultured *in vitro*. We treated the cells with two independent pro-hypertrophic stimuli, phenylephrine (PE) and insulin-like growth factor 1 (IGF1), to induce cardiomyocyte growth. By RNA-seq analysis, a total of 1,821 genes showed significant changes by PE, while IGF1 treatment altered 1,313 genes (Figures 1B and S1A). We focused on the overlapping 347 (213 upregulated, 134 downregulated) genes for further analysis. Ingenuity pathway analysis (IPA) showed that metabolic process was the top altered pathway by hypertrophic stimulation (Figure 1C). Since glucose utilization has been shown to play a critical role in cardiac hypertrophic growth (Ritterhoff and Tian, 2017), we focused on genes related to this pathway (Figure 1D). Importantly, we found that most enzymes of glycolysis showed significant changes by either PE or IGF1 treatment (Figure S1B). Indeed, when glycolytic rate was analyzed, we found that PE treatment led to a significant increase in glycolysis (Figures 1E and S1C).

Lactate dehydrogenase (LDH) is a tetrameric enzyme catalyzing the conversion between pyruvate and lactate (Gladden, 2004). Two homologous proteins, LDHA and LDHB, form LDH isoforms with five different combinations (i.e., A4, A3B1, A2B2, A1B3, and B4). While the A4 isoform is more glycolytic, the B4 tetrameric enzyme mainly catalyzes the conversion from lactate to pyruvate for oxidation. Here, we found that PE treatment led to significant upregulation of LDHA in NRVMs as early as 6 h after administration (Figures 1F and 1G). Immunofluorescence staining confirmed the induction of LDHA by PE (Figure 1H). Consistently, endothelin-1 (ET-1), another widely used hypertrophic stimulus, similarly increased LDHA expression in NRVMs (Figures S1D and S1E).

At the *in vivo* level, thoracic aortic constriction (TAC) is a commonly used surgical approach to induce pressure overload and trigger cardiac hypertrophic growth (Hill et al., 2000). In response to elevated afterload stress, the heart manifests cardiac hypertrophy to ameliorate ventricular wall stress (Wang et al., 2017). We subjected wild-type C57BL/6 mice to TAC and harvested the heart 1 week later. We have shown previously that this surgical procedure leads to significant and consistent cardiac hypertrophic growth (Tran et al., 2020; Wang et al., 2019; Zhang et al., 2019). Here, LDHA was augmented in the heart by TAC at protein, mRNA, and histological levels (Figures 1I–1L). We next used an in-gel LDH enzymatic activity assay to assess the distribution of different tetrameric LDH isoforms. Importantly, cardiac hypertrophic growth was associated with an increase in the isoforms with more LDHA (Figure 1M). We went on to examine LDHA activity by measuring glycolytic intermediates using mass spectrometry (MS) (Figures S1F and S1G). Consistent with the elevation of LDHA expression and its enzymatic activity, cardiac hypertrophic growth was accompanied by an increase in cardiac lactate level (Figures 1N and S1H). Taken together, these results suggest that both expression and activity of LDHA are significantly elevated by hypertrophic growth in the heart.

LDHA Is Required for Cardiac Hypertrophic Growth in Response to Pressure Overload *In Vivo*

We went on to investigate the role of LDHA in cardiac hypertrophic growth *in vivo*. We took advantage of cardiac-specific knockout (KO) of LDHA by crossing the $LDHA^{F/F}$ model (Wang et al., 2014a) with a cardiomyocyte-restricted Cre transgenic mouse line (αMHC-Cre). In the conditional KO (cKO) mice, LDHA was eliminated from the heart (Figures S2A and S2B).

We then subjected the cKO mice along with littermate controls to pressure overload by TAC and followed cardiac function over time (Figure S2C). LDHA deficiency under hemodynamic stress led to impairments in cardiac systolic performance, as revealed by decreases in both fractional shortening and ejection fraction (Figure 2A). No changes in heart rate were noticed (Figure S2D), while both diastolic and systolic LVIDs (left ventricular internal diameters were significantly elevated in the cKO mice (Figures S2E and S2F). However, no differences in mortality were identified (data not shown). These findings suggest that deficiency of LDHA in the heart deteriorates cardiac response to pressure overload.

After 1 week of TAC, the control LDHF/F mice showed significant upregulation of heart weight (Figures 2B and S2G) with a concomitant increase in cardiomyocyte size (Figure 2C). This augmentation was, however, diminished in the cKO mice (Figures 2B, 2C, and S2G). These results indicate that LDHA is required for cardiac hypertrophic growth in response to pressure overload. Consistent with the role of LDHA in forming different LDH isoenzymes, deletion of LDHA caused a strong decrease of LDH isoforms containing LDHA (Figure S2H). Molecular markers of cardiac hypertrophy such as Anf and Bnp were significantly upregulated by TAC, and these increases were attenuated after LDHA elimination (Figure 2D). Importantly, LDHA deficiency in the heart caused cell death and severe fibrosis after long-term pressure overload, which might be an underlying reason of reduced contractility (Figures S3A and S3B). To further delineate the changes in LDHA cKO hearts, we examined cardiac metabolism using labeled nutrients to determine glucose/lactate/pyruvate oxidation and fatty acids β-oxidation, respectively (Figures S3C–S3E). Pressure overload led to a trend of increase in glycolytic flux rate, which was partially reduced by LDHA deficiency (Figure S3F). Consistent with the elevation of glucose utilization, long-chain fatty acid oxidation was decreased in the TAC heart, and this change was reverted by LDHA deletion (Figure S3G). In particular, the oxidation of lactate/pyruvate was severely diminished. The ratio of lactate/ pyruvate to long-chain fatty acids was therefore reduced in LDHA KO hearts (Figure S3H). Taken together, these results suggest that cardiomyocyte LDHA is required for the heart to mount an adaptive growth response under pressure overload.

LDHA Is Necessary and Sufficient to Drive Cardiomyocyte Growth

After showing the requirement of LDHA in cardiac hypertrophic growth *in vivo*, we sought to address the role of LDHA in cardiomyocytes in a cell-autonomous manner. We silenced LDHA expression in NRVMs by small interfering RNA (siRNA) transfection (Figures S4A–S4C). We then treated the cells with PE for 24 h. We confirmed that PE treatment increased LDH isoenzymes containing LDHA, and LDHA silencing reverted this trend (Figure S4D). Interestingly, we found that LDHA knockdown led to a decrease in mitochondrial respiration (Figures S4E and S4F). Cardiomyocyte size was significantly increased by PE stimulation, and this effect was strongly diminished by LDHA knockdown (Figure 3A). Next, we included a trace amount of radioactively labeled leucine (^{3}H-leucine) in the culture medium. Cardiomyocyte protein synthesis as determined by leucine incorporation was elevated by PE treatment (Figure 3B). Consistent with the decrease in cell size, silencing of LDHA significantly reduced leucine incorporation (Figures 3A and 3B). At the molecular level, knockdown of LDHA led to a decrease in hypertrophic marker gene expression (Figure 3C). Further experiments using another independent siRNA against LDHA showed similar findings (Figures S4A–S4C and S4G– S4I).

We next evaluated the role of LDHA in cardiac growth with a pharmacological approach. FX11 is a cell-permeable, selective inhibitor of LDHA (Le et al., 2010). Inclusion of FX11 for up to 5 mM did not significant affect viability of NRVMs (data not shown). We found that FX11 of as low as 1 μM strongly suppressed cardiomyocyte growth stimulated by PE (Figure S4J), which was confirmed by decreases in leucine incorporation and fetal gene

expression (Figures S4K and S4L). Collectively, these findings suggest that LDHA expression and activity play a critical role in cardiomyocyte growth *in vitro*.

We next asked whether overexpression of LDHA is sufficient to drive cardiomyocyte growth. We generated adenovirus expressing either GFP control or LDHA (Figure 3D). After infection of NRVMs, we assessed cell size. Importantly, we found that overexpression of LDHA led to a significant increase in cardiomyocyte size (Figure 3E). Radioactive leucine incorporation was similarly augmented by LDHA overexpression (Figure 3F). These data together suggest that LDHA induction is sufficient to drive cardiomyocyte growth.

LDHA-Derived Lactate Potentiates Cardiomyocyte Hypertrophic Growth

LDH catalyzes the conversion between pyruvate/NADH and lactate/NAD^+. Deficiency of LDHA causes the decrease of lactate and NAD+, which may mediate the growth defect in cardiomyocytes. To address the role of lactate in LDHA-associated cell growth, we first determined cellular lactate production. PE-induced cardiomyocyte hypertrophic growth in NRVMs was accompanied by a significant increase in cellular lactate level as measured by MS (Figure 4A). Consistent with the role of LDHA, knockdown led to a decrease of cellular lactate (Figure 4B). We next asked the question of whether supplementation of lactate could rescue the defect in cell growth from LDHA silencing. To address it, we first reduced LDHA expression by siRNA transfection, followed by PE treatment. We supplemented lactate in the culture medium to increase the cellular lactate level in NRVMs (Figure S5A). Importantly, lactate treatment alone was sufficient to increase gene expression of hypertrophic markers (Figure S5B). Moreover, we found that lactate treatment significantly rescued the defect in cell growth from LDHA silencing (Figures 4C and 4D). Leucine incorporation assay confirmed this lactate-mediated rescue effect (Figure 4E). Consistently, molecular markers of hypertrophy were restored by lactate supplementation under the condition of LDHA silencing (Figures 4F and 4G). Collectively, these findings indicate that lactate production from LDHA stimulates cardiomyocyte hypertrophic growth.

NAD^+ is the other product from the LDHA-catalyzed reaction. To delineate the contribution of NAD+ in LDHA-mediated hypertrophic growth, we silenced LDHA by siRNA in NRVMs and then treated the cells with NMN (nicotinamide mononucleotide), a precursor for NAD^+ biosynthesis (Rajman et al., 2018). Supplementation of NMN did not rescue the cardiomyocyte growth defect (Figures S5C and S5D) or restore Rcan1.4 protein expression (data not shown), a hypertrophic growth marker, even though intracellular NAD^+ level was significantly elevated (Figure S5E). These data together suggest that NAD^+ may not be involved in LDHA-triggered cardiomyocyte growth, highlighting the important role of lactate.

NDRG3 Expression Is Augmented by LDHA

Our results suggest that lactate as a metabolic product of LDHA might directly promote cardiomyocyte growth. We next sought to determine the underlying mechanism. NDRG (N-myc downregulated gene family) belongs to the α/β hydrolase superfamily, which participates in stress responses, cell growth, and differentiation (Melotte et al., 2010). However, its role in cardiac hypertrophic growth remains to be determined. A recent study

shows that lactate specifically binds NDRG3 and stabilizes its protein level under hypoxic conditions (Lee et al., 2015). Moreover, elevation of NDRG3 leads to activation of c-Raf and ERK (extracelluar signal-regulated kinase) and improves cell survival. Considering the important roles of lactate and ERK in cardiac hypertrophic growth, we set up to investigate the relationship between lactate and NDRG3 in cardiomyocytes.

We found that NDRG3 was significantly elevated in cultured cardiomyocytes after stimulation by PE (Figures 5A and S5F) or ET-1 (Figure S5G) and in hypertrophic hearts after TAC (Figure 5B). Lactate treatment alone was sufficient to increase NDRG3 expression at the mRNA level (Figure S5B). Importantly, siRNA-mediated knockdown of LDHA in NRVMs led to a decrease in NDGR3 expression (Figure 5C), and this decrease was rescued by supplementation of lactate in culture media (Figure 5D). Further, suppression of LDHA enzymatic activity in NRVMs by FX11 caused a decrease of NDRG3 expression (Figure S5H). Additionally, PE-induced augmentation of NDRG3 was reduced by LDHA silencing (Figure S5I). In contrast, overexpression of LDHA in NRVMs by adenovirus infection increased NDRG3 protein expression (Figure 5E). Consistent with these *in vitro* findings, TAC-induced hypertrophic growth in the heart was accompanied by elevation of NDRG3 expression, which was diminished by LDHA KO (Figure 5F). Taken together, these data suggest that cardiomyocyte LDHA may govern the expression of NDRG3 in the heart.

We went on to assess the role of NDRG3 in cardiomyocyte hypetrophic growth. We found that NDRG3 silencing suppressed PE-induced cardiomyocyte growth (Figures 5G and S5J). The leucine incorporation assay confirmed this finding (Figure 5H). Consistently, molecular markers of cardiac hypertrophic growth were augmented by PE treatment, which was inhibited by NDRG3 silencing (Figure 5I). In addition, another independent siRNA against NDRG3 showed similar findings (Figures S5J– S5M). These results indicate that NDRG3 is required for cardiomyocyte hypertrophic growth.

We next asked whether overexpression of NDRG3 is sufficient to drive hypertrophic growth. We generated adenovirus to express NDRG3 and infected NRVMs. Overexpression of NDRG3 was sufficient to increase cardiomyocyte size to a degree similar to PE treatment (Figure S6A). Interestingly, PE treatment did not lead to a further increase in cell size (Figure S6A). These findings were then confirmed by the leucine incorporation assay (Figure S6B). At the cellular level, NDRG3 overexpression caused an increase in the expression of hypertrophic molecular markers (Figure S6C). Taken together, these results suggest that NDRG3 is necessary and sufficient to drive cardiomyocyte growth.

NDRG3 Is Required for LDHA-Mediated Hypertrophic Growth

Since NDRG3 may be a downstream target of LDHA-derived lactate, we next asked whether NDRG3 is required for LDHA-related cardiomyocyte growth. Overexpression of LDHA in NRVMs was sufficient to drive cell growth, and importantly, this elevation was reduced by NDRG3 silencing (Figure 6A). Expression pattern of hypertrophic markers confirmed these findings (Figure 6B). On the other hand, lactate supplementation could rescue LDHA-silencing-caused decrease in cell growth. However, this rescue was completely prevented by NDRG3 silencing (Figures 6C and 6D). Consistent with the essential role of NDRG3 in

mediating the action of the LDHA/lactate axis, knockdown of NDRG3 inhibited protein expression of both Anf and βMHC, two hypertrophic molecular markers (Figure S6D). Collectively, these findings suggest that NDRG3 is augmented by the LDHA/lactate axis, which is required for LDHA-mediated cardiomyocyte growth.

The LDHA/NDRG3 Axis Activates ERK in Cardiac Hypertrophic Growth

ERK is a serine/threonine kinase involved in numerous signaling pathways, including growth, mitosis, and cell differentiation (Lawrence et al., 2008). Previous studies have shown that ERK exerts essential roles in cardiac hypertrophic growth and HF (Kehat and Molkentin, 2010).

To evaluate the relationship between ERK and the LDHA/ NDRG3 axis, we first examined the activation of ERK under cardiac hypertrophic growth. In cultured NRVMs, both PE and ET-1 treatments stimulated ERK phosphorylation (Figures S7A and S7B). Consistently, pressure overload by TAC led to activation of ERK in the heart (Figure S7C). Interestingly, LDHA silencing by siRNA or inhibition by enzymatic inhibitor FX11 was associated with a decrease of ERK phosphorylation (Figures S7D and S7E). Moreover, lactate treatment led to an additional increase in ERK phosphorylation compared to PE alone (Figure S7F). At the *in vivo* level, LDHA KO in the heart significantly suppressed ERK phosphorylation after pressure overload (Figure S7G). Collectively, these data suggest that LDHA is required for ERK activation during cardiomyocyte hypertrophic growth.

We went on to evaluate the role of NDRG3 in ERK activation. Overexpression of LDHA led to an increase in ERK phosphorylation, which was significantly suppressed by NDRG3 silencing (Figure 7A). Further, knockdown of NDRG3 caused a decrease in ERK activation after PE treatment (Figure 7B). On the other hand, overexpression of NDRG3 potentiated PE-induced activation of ERK (Figure 7C). These results indicate that NDRG3 may directly activate ERK in NRVMs. To further delineate the relationship among LDHA/NDRG3, ERK, and cardiomyocyte growth, we treated NRVMs with U0126, an ERK inhibitor (Favata et al., 1998). LDHA overexpression stimulated ERK, which was inhibited by U0126 (Figure 7D). Importantly, suppression of ERK by U0126 led to a significant decrease in the expression of hypertrophic markers (Figure 7D).

Previous studies show that NDRG3, when binding lactate, interacts with c-Raf and activates the latter (Lee et al., 2015). Here, consistent with the activation of ERK, overexpression of NDRG3 in NRVMs led to a significant increase in c-Raf phosphorylation (Figure S7H). On the other hand, silencing of LDHA caused a decrease in NDRG3 expression, which was accompanied by a reduced signal of phosphorylated c-Raf (Figure S7I). At the *in vivo* level, cardiac-specific LDHA knockout strongly decreased c-Raf phosphorylation (Figures S7J and S7K). Taken together, these results suggest that the LDHA/NDRG3 axis plays a critical role in regulating c-Raf/ERK and cardiac hypertrophic growth in response to pressure overload.

DISCUSSION

HF is a leading cause of morbidity and mortality worldwide. High blood pressure is one of the most important etiologies of HF (Benjamin et al., 2019). Because of the high incidence rate and prevalence of hypertension, HF has become an epidemic. In response to elevated blood pressure, cardiac ventricular wall stress is augmented. As a consequence, the heart manifests hypertrophic growth to accommodate the stress and maintain pumping function. This growth response, once required for adaptation, may decompensate and succumb to HF under persistent hemodynamic stress. The underlying mechanism of cardiac growth and the transition to HF remains incompletely characterized. Here, we show that LDHA plays an essential role in adaptive hypertrophic growth. Deficiency of LDHA in cardiomyocytes in the heart leads to defective cardiac hypertrophy and precipitated development of HF. At the mechanistic level, lactate as a product of LDHA mediates its action in stimulating NDRG3 and activating the pro-growth ERK signal. These findings highlight the importance of the LDHA/lactate/NDRG3 axis in the heart in governing cardiac hypertrophic growth in response to elevated blood pressure.

Metabolic Remodeling in Pathological Cardiac Hypertrophy

In response to pressure overload, the heart shows pathological cardiac remodeling at various levels. Previous studies have shown that metabolic remodeling precedes most if not all other alterations in the heart, which may play a causative role in cardiac hypertrophic growth (Kundu et al., 2015; Nakamura and Sadoshima, 2018). The adult heart mainly catabolizes fatty acids for energy production, with less contribution from oxidation of glucose and lactate. Under the hypertrophic condition, however, the proportion of glucose utilization in ATP generation is significantly elevated (Stanley et al., 2005). Along this line, multiple genes in the glucose utilization pathway are increased by pressure overload, including HIF1-α, GLUT1, HK1, and PFK (Nascimben et al., 2004; Sano et al., 2007). This important feature of cardiac metabolism in hypertrophy resembles characteristics of the heart during development. Indeed, Lopaschuk et al. (1991) showed that glycolysis is a predominant source of ATP production in the heart immediately after birth. Importantly, the contribution of glycolysis to energetics in hypertrophic hearts is increased by 3-fold compared to sham hearts (Allard et al., 1994). This metabolic remodeling belongs to the so-called fetal gene program, which is maintained at a low level in adult hearts but re-activated during cardiac remodeling (Taegtmeyer et al., 2010). While many genes of cardiac metabolic remodeling are used as molecular signatures for this process, their roles and significance are not fully understood.

Metabolic remodeling may play an important role in cardiac hypertrophic growth, above and beyond a molecular marker. Glucose metabolism may contribute to cardiac hypertrophy via at least two mechanisms. First, elevated glycolysis as a convenient route for glucose catabolism can produce necessary ATP for cardiomyocytes to maintain essential pump functions during growth. On the other hand, catabolic intermediates from glycolysis may be shunted to biosynthetic pathways to fulfill the requirements of cardiomyocyte enlargement (Umbarawan et al., 2018). The increase of glucose metabolism may therefore help maintain cardiac function under hemodynamic stress (Doenst et al., 2013). Indeed, Tian and

colleagues show that overexpression of GLUT1 in cardiomyocytes leads to an increase in glycolysis and, importantly, improvements in cardiac performance under chronic pressure overload (Liao et al., 2002).

LDHA in Pathological Cardiac Remodeling

LDH activity is much higher than that of other enzymes of glycolysis and glucose oxidation (Rogatzki et al., 2015). Moreover, the LDH-catalyzed reaction has a high lactate-leaning equilibrium constant. Therefore, lactate is always the end product of glycolysis under essentially all metabolic conditions. However, lactate has long been considered a metabolic waste of glycolysis due to hypoxia and a major cause of muscle fatigue. Emerging evidence strongly suggests lactate can no longer be considered the suspect of metabolic crimes but is an essential player in energy homeostasis as a significant fuel source, a precursor for gluconeogenesis, and a signaling molecule (Brooks, 2018; Gladden, 2004). Faubert et al. (2017) found that circulating lactate is a significant substrate for tricarboxylic acid (TCA) cycle in human non-small-cell lung cancers. *In vivo* metabolomics assay shows that lactate is a predominant source for energy production compared with glucose. Consistently, genetic deletion of LDHA suppresses tumorigenesis and decelerates disease progression of lung cancer (Xie et al., 2014). Targeting LDHA therefore represents a promising avenue for cancer treatment (Doherty and Cleveland, 2013).

LDHA and LDHB are encoded by two separate genes, which form LDH enzymes of different combinations. While LDH1 consists of four LDHB subunits (the heart form), LDH5 is assembled by four LDHA monomers (the muscle form). Although LDH catalyzes a reversible reaction between pyruvate and lactate, the LDH isoenzymes with more LDHA may facilitate the production of lactate. Under various disease conditions, including tumorigenesis, ischemic insults, and so forth, LDHA expression is elevated. As a consequence, the LDH isoenzymes with more LDHA are increased, which likely contributes to the augmentation of glycolysis and lactate production. Indeed, changes in LDHA and LDH isoenzymes have been appreciated for decades during cardiac hypertrophic growth and HF. Early studies by Stagno and colleagues show that muscle-type LDH is significantly induced across four different models of hypertrophy, including high altitude, aortic stenosis, swimming, and running (York et al., 1976). In addition, a rabbit study by Revis and Cameron (1978) found that constriction of abdominal aorta induces cardiac hypertrophy, which is accompanied by an increase of the ratio between muscle and heart types of LDH. These findings have been confirmed in rats by partial abdominal aorta constriction (Zhang et al., 1998). Moreover, a human study shows a trend of increasing LDH in patients with hypertrophic cardiomyopathy in comparison with creatine kinase-MB, and the latter is largely considered a marker of cardiac injury (Hamada et al., 2016). One potential underlying mechanism of the elevation of muscle-type LDH may involve induction of miR375–3p that targets LDHB (Feng et al., 2019). Despite a strong association between LDHA and related isoenzymes in cardiac hypertrophic growth, its role and underlying mechanisms remain to be fully characterized.

Previous studies have shown that glucose uptake and glycolysis are significantly elevated in the heart during hypertrophic growth, while glucose oxidation via the TCA cycle is largely

maintained (Leong et al., 2003). These findings raise a possibility that the increased cardiac lactate may participate in other actions, except being excreted from cardiomyocyte. Lee et al. (2015) found that lactate in cancer cells may directly interact with NDRG3 and stabilize the latter, which is essential to stimulate the pro-survival ERK signaling. This molecular mechanism operates under hypoxic conditions, and the lactate/NDRG3 nexus may corroborate with the HIF1-α signaling to ensure surviving advantages in cancer cells. In addition, Zhang and colleagues show that vascular smooth muscle cells assume a synthetic phenotype by upregulation of lactate production and stimulation of NDRDG3 in response to hypoxia (Yang et al., 2017). Here, we found that LDHA upregulation and lactate elevation enhance the expression of NDRG3 and activate an adaptive growth response in the heart. Defects in this pathway may contribute to decompensation of cardiac hypertrophic growth and accelerate the development of HF. Additionally, other adaptive changes from LDHA deficiency in the heart may not be excluded, including alterations in LDHB. Phenotypic contributions from these adaptations may be addressed by using distinctive ^{13}C labeling patterns in the various sources of pyruvate.

The acute, adaptive response under pressure overload is essential for the heart to maintain cardiac function. Previous studies of eliminating mTOR in cardiomyocytes show that cardiac performance quickly progresses into cardiomyopathy and dilation by pressure overload (Zhang et al., 2010). Here, we found that LDHA is required for cardiac response to pressure overload, and deficiency of LDHA in the heart causes cardiomyopathy from defective cardiac hypertrophy. However, caution needs to be exercised when speculating the translational potential of these findings. Ample evidence shows that LDHA is upregulated during tumorigenesis and suppressing LDHA has been a promising approach to targeting cancer. Therefore, activation of LDHA that may benefit the adaptive cardiac response under hemodynamic stress could lead to unwanted effects of malignancies. A better and more appropriate means may be time-and tempo-specific manipulation of LDHA under different disease contexts.

Conclusions and Future Perspectives

Cardiac metabolic remodeling is an essential component in cardiac hypertrophic growth. LDHA, as a key player in glucose metabolism, is significantly upregulated by pressure overload in the heart. Importantly, cardiomyocyte-restricted knockout of LDHA causes defective heart growth and early development of cardiac dysfunction, highlighting a critical role of LDHA in adaptive cardiac growth. Mechanistically, lactate as a product of LDHA mediates the pro-growth function by stimulating NDRG3 and ERK. Future work may be warranted to dissect the interaction between lactate and NDRG3 and the contribution of ERK-c-Raf signaling in lactate-mediated growth. Taken together, our findings uncovered an important role of LDHA in governing cardiac hypertrophic growth under hemodynamic stress, which may represent a new target for future therapeutic explorations against hypertensive heart disease.

STAR★METHODS

RESOURCE AVAILABILITY

Lead Contact—Further information and requests for resources and reagents should be directed to and will be fulfilled by the Lead Contact, Zhao Wang (zhao.wang@utsouthwestern.edu).

Materials Availability—All unique reagents generated in this study are available from the Lead Contact with a complete Material Transfer Agreement.

Data and Code Availability—The RNA-seq datasets generated during this study are available at the Gene Expression Omnibus under GEO: GSE153763.

EXPERIMENTAL MODEL AND SUBJECT DETAILS

Animal models—All animal experiments were approved by The Institutional Animal Care and the Use Committee of University of Texas Southwestern Medical Center (UTSW). Mice were housed at constant temperature with a 12 hour light-dark cycle. Mice were fed standard rodent chow diet (2916, Teklad) with free access to water. The conditional $LDHA^{F/F}$ mice (C57BL/6 background) (Wang et al., 2014a) were crossed to α-MHC-Cre transgenic mice to generate the cardiomyocyte-specific LDHA conditional knockout (cKO) mouse model. Genotyping information is provided in Table S1.

Wild-type male mice or genetically modified animals of 8–10 weeks old were used for thoracic aortic constriction (TAC) surgery as previously described (Wang et al., 2017; Zhang et al., 2019). Briefly, mice were anesthetized by intraperitoneal injection of ketamine (100 mg/kg body weight) and xylazine (5 mg/kg body weight). The left chest was opened to identify the thoracic aorta when the mouse had no toe-pinch reflex. A 27-gauge needle with 5–0 silk sutures was used to ligate the thoracic aorta. Adequate constriction of the aorta was induced and confirmed by Doppler echocardiography (data not shown). The needle was then removed before the chest was closed. Sham control mice underwent the same surgical procedure without transverse aortic banding. The surgery was done in a blinded manner and the surgeon did not know genotypes and treatments.

Echocardiography was performed by using the Vevo 2100 High-Resolution Micro-Imaging System (VisualSonics) with a MS400C ultrasound transducer as described previously (Tran et al., 2020; Wang et al., 2019; Zhang et al., 2019). The short-axis view of left ventricle at the level of the papillary muscles was captured and M-mode recordings were performed. Various parameters including interventricular septum thickness (IVS), heart rate (HR), left ventricular posterior wall thickness (LVPW), and left ventricular internal diameter (LVID) at both end-diastole and end-systole were determined. Ejection fraction (EF) and fractional shortening (FS) was then calculated.

Culture of Neonatal rat ventricular myocytes (NRVMs)—NRVMs were isolated from 1–2 days old Sprague-Dawley rats (Charles River) as previously described (Bi et al., 2018; Wang et al., 2014b). Immunofluorescence staining for α-actinin is conducted for each preparation, and cardiomyocyte purity is approximate 85%. NRVMs were plated in 6-well or

12-well plates at a density of 1,250 cells/mm^2 and cultured in Dulbecco's modified Eagle's medium (DMEM) /M199 (3:1) containing 5% fetal bovine serum (FBS), 10% horse serum, and 100 mM BrdU (19160, Sigma-Aldrich). Cells were then cultured with serum-free DMEM/M199 (3:1) for 24 hours prior to various treatments.

METHOD DETAILS

Gene knockdown by siRNA—NRVMs were transfected with siRNA oligos (Sigma) using Lipofectamine RNAiMAX (13778150, ThermoFisher) in Opti-MEM for 6 hours. The medium was then replaced by fresh serum-free DMEM/M199 (3:1). Mission siRNA universal negative control #1 (SIC001, Sigma) was used as a negative control. Various treatments were performed at 24 hours after knockdown. For hypertrophy stimulation, NRVMs were exposed to serum-free DMEM/M199 (3:1) containing phenylephrine (PE, 50 μM), endothelin-1 (ET-1, 20 nM), insulin-like growth factor 1 (IGF1, 10 nM), or corresponding vehicles for 6, 12 or 24 hours, respectively.

Adenovirus production, purification, and transduction—Full-length mouse LDHA and NDRG3 genes were amplified from a mouse heart cDNA library and subcloned into an adenovirus expression vector using the Adeno-X Adenoviral System 3 (CMV promoter and Zsgreen1 reporter, Takara). The adeno-X 293 cell line was purchased from Takara (632271). Adenovirus expressing LDHA or NDRG3 was harvested from culture supernatants and cell lysates. NRVMs were then transduced using GFP-only adenovirus as a negative control, and the cells were collected 24 or 48 hours after infection.

RNA isolation, RNA-seq analysis, and real-time RT-PCR—Total RNA was isolated from cardiac tissues and NRVMs using the Total RNA Fatty and Fibrous Tissue kit (7326830, Bio-Rad) and the Quick-RNA MicroPrep kit (R1055, Zymo Research), respectively.

RNA-seq analysis was conducted by the Macrogen Clinical Laboratory. Gene fold changes were analyzed by filtering the dataset with arbitrary fold change (FC) cut-offs of > 1.4 and a p value < 0.01 using ANOVA statistical analysis. Pathway analysis was done with Ingenuity Pathway Analysis (IPA) (Ingenuity Systems).

For quantitative PCR, cDNA was prepared from 250 ng total RNA using the iScript Reverse Transcription Supermix (1708841, BioRad). Real-time PCR was performed with SYBR Green (B21203, Bimake) on a LightCycler (Roche) or CFX96/384 (Bio-Rad) system. Relative mRNA levels were calculated by using the $2^{-\Delta\Delta Ct}$ method and normalized to 18 s RNA. All primers are provided in Table S1.

^{3}H-leucine incorporation—NRVMs were cultured with radioactive L-3,4,5-^{3}H-leucine (NET460A001MC, PerkinElmer) at a final concentrations of 2 μCi/mL. After 24 hours of treatment, the cells were washed for 3 times with ice-cold phosphate-buffered saline (PBS) and incubated with 10% trichloroacetic acid (LC262302, 2 mL/well, LabChem) for 30 minutes at 4°C with gentle agitation, followed by two washes with ice-cold 95% ethanol. Samples were incubated with 1 mL NaOH (0.5 N) for overnight at 37°C with gentle agitation, and then neutralized with 1 mL HCl (0.5 N). Finally, all content was transferred to

a scintillation vial, followed by mixing with 18 mL scintillation solution (882475, EcoLite, MP Biomedicals) for radioactivity detection (LS5000TA, Beckman).

Histological and immunohistochemical analyses—Mouse hearts were harvested and immediately fixed in 10% neutralized formalin for 48 hours. Paraffin sections of 5-μm thickness were used. Hematoxylin and eosin (H&E) staining and Masson's Trichrome staining were performed by the Molecular Pathology Core at UTSW.

For fluorescent immunostaining in cardiac tissues, sections were first deparaffinized and rehydrated. Antigens were retrieved using antigen retrieval citrate solution (HK086–9K, BioGenex), and then permeabilized with 0.1% Triton X-100/PBS for 30 minutes at room temperature. All slides were blocked for 1.5 hours using 5% normal goat serum. Primary antibodies against LDHA (anti-rabbit, 1:100, 2012, Cell Signaling Technology), p-c-Raf (anti-mouse, 1:100, SC-271929, Santa Cruz Biotechnology), NDRG3 (anti-rabbit, 1:100, 5846, Cell Signaling Technology), and α-actinin (anti-mouse, 1:200, A7732, Sigma) were used to incubate overnight. Sections were then washed with PBS for 4 times and stained with corresponding secondary antibodies (goat anti-rabbit secondary antibodies Alexa Fluor 488, or goat anti-mouse secondary antibodies Alexa Fluor 568, ThermoFisher) for 1 hour at room temperature. After 6 washes with PBS, sections were counterstained by the ProLong Gold antifade reagent with DAPI (4,6-diamidino-2-phenylindole) (P36931, ThermoFisher). Images were captured by a fluorescent (Leica) or confocal (Zeiss) microscope.

For wheat germ agglutinin (WGA) staining, transverse heart sections were deparaffinized and rehydrated. Antigen retrieval was then conducted. Slices were stained with Alexa Fluor 594-conjugated WGA (W11262, 10 mμg/mL, ThermoFisher) for 1 hour at room temperature. After mounting with the ProLong Gold antifade reagent (P36931, ThermoFisher), sections were imaged using a fluorescence microscope (Leica). Cardiac myocytes with circularity coefficient of more than 0.75 were chosen and cell size was quantified using ImageJ software.

For fluorescent immunostaining *in vitro*, NRVMs were cultured in 12-well plates with coverslips. After treatments, cells were fixed with 4% paraformaldehyde for 20 minutes and permeabilized with 0.1% Triton X-100 for 10 minutes before incubation with primary antibodies. After 6 washes with PBS, the cells were stained with corresponding secondary antibodies for 1 hour. NRVMs were then sealed with the ProLong Gold antifade reagent with DAPI (4,6-diamidino-2-phenylindole) (P36931, ThermoFisher) and imaged with a fluorescent (Leica) or confocal (Zeiss) microscope.

ECAR analysis—Extracellular acidification rate (ECAR) analysis in NRVMs was performed using the XF24 Extracellular Flux Analyzer (Seahorse Bioscience) as previously described (Readnower et al., 2012). Briefly, 75,000 NRVMs were plated in a coated XF24 cell culture microplate with 100 μL standard culture media, and treated with PE (50 μM) at 37°C in a 5% CO_2 incubator for 24 hours. NRVMs were then washed with XF media twice and incubated in CO_2-free incubator at 37°C for 1 hour. Oligomycin (1 μM), FCCP (1 μM), and Rotenone (100 nM)/Antimycin A (10 μM) were then used to treat the cells and ECAR was determined.

NMR isotopomer analysis of cardiac metabolism—^{13}C-NMR isotopomer analysis was carried out to evaluate the substrate competition between glucose and fatty acids in isolated Langendroff perfused mouse hearts from sham and TAC mice. We chose the time of 1-week post surgery to avoid confounding issues from cardiac dysfunction of later stages. Here, only LDHA$^{F/F}$ and cKO after TAC were used to compare with control sham animals since no phenotypical differences were found between LDHA$^{F/F}$ and cKO at baseline. Following cervical dislocation, mouse hearts were excised, cannulated via aorta, and then connected to a perfusion column apparatus maintained at 37°C in a controlled temperature bath. The hearts were retrograde perfused for 30 minutes at 80 cm H_2O pressure with a modified Krebs-Henseleit (KH) buffer containing 8 mM [1,6-^{13}C]glucose, 1.2 mM [2-^{13}C]lactate, 0.12 mM [2-^{13}C]pyruvate, 0.63 mM [U-^{13}C]long chain fatty acids (LCFA) with 0.75% bovine serum albumin (BSA), and 50 μU/mL insulin. The non-recirculating buffer was oxygenated with a thin-film oxygenator with a 95:5 mixture of O_2:CO_2. Heart rate was recorded throughout the perfusion with a fluid-filled catheter in the left ventricle. Oxygen consumption was measured by collecting coronary flow samples into a gas-tight syringe at 5 and 25 minutes and analyzed using a blood gas analyzer (Instrumentation Laboratory). Hearts were then snap-frozen immediately after 30 minutes of perfusion, pulverized in liquid nitrogen, and extracted with perchloric acid (4%). Perchloric extracts of heart tissues were then neutralized, and reconstituted in D_2O containing 1 mM ethylenediaminetetraacetic acid (EDTA) and 0.5 mM 2,2-dimethyl-2-silapentane-5-sulfonate (DSS) standard. Proton-decoupled ^{13}C-NMR spectra of heart extracts were acquired at 14.1 T spectrometer (Bruker Corporation), equipped with 5-mm cryoprobe. ^{13}C NMR multiplets from glutamate were deconvoluted using ACD/SpecManager (ACD Labs) and multiplet ratios were used to calculate the relative oxidation of [1,6-$^{13}C_2$]glucose, [2-^{13}C]lactate-[2-^{13}C]pyruvate, [U-^{13}C]FA, and unlabeled endogenous substrates (e.g., triglycerides and glycogen).

LC-MS/MS analysis—The hearts were washed for 5 s in ice-cold PBS to remove excess blood and metabolites, snap-frozen in liquid nitrogen, and stored at −80°C until further use. For metabolite extraction, 10–15 mg of left ventricle was weighed and put into a 5 mL tube containing 1 mL of methanol/water (80:20, vol/vol). The tissues were homogenized for 2 minutes. Homogenate (400 mL) was transferred to a tube prefilled with 800 μL of ice-cold methanol/water (80:20, vol/vol) (pre-cooled at −80°C). The homogenate was mixed rigorously for 1 minute, and then centrifuged at 14,000 rpm for 15 minutes. Supernatant of 900 μL was transferred into a new tube. The pellet was then resuspended with 500 μL ice-cold methanol/water (80:20, vol/vol) for second extraction. A total of 1,400 μL supernatant was collected and dried under vacuum at 37°C. The pellet was stored at −80°C until analysis. Three technical replicates of each sample were performed. Level of metabolite was normalized to tissue weight.

To examine the metabolites in NRVMs, culture medium was aspirated and cells were rinsed in cold PBS after different times of PE treatment. Cells were then lysed in 0.5 mL of cold 80% methanol (pre-cooled at −80°C), with three cycles of freezing-thawing between liquid nitrogen and 37°C water. The lysates were cleared of debris by centrifugation, and metabolites in the supernatant were concentrated by centrifugation under vacuum. The dried

pellet was stored at −80°C until analysis. Three technical replicates of each sample were used. Metabolite level was normalized to total proteins in mg.

Metabolite quantification was carried out on a Shimadzu LCMS-8040 triple quadrupole mass spectrometer. The instrument was operated and optimized with negative electrospray ionization in multiple reaction mode (LC-MS/MS–ESI MRM). The analytes were separated on a Sepax 3 μm C-18 150 X 2.1 mm column (Sepax Technologies) using a Shimadzu Nexera LC-30AD Ultra High Performance Liquid Chromatograph system and a SIL-30AC autosampler (Shimadzu Corporation). The mobile phases used were: A) 0.185% tributylamine (TBA) and 0.13% acetic acid in water and B) 0.13% in methanol at the flow rate of 0.2 mL/minute. The LC gradient program was as the following: 0–10 minutes, 25% B; 10–25 minutes, 75% B; 25–26 minutes, 75%–95% B; 26–36 minutes, 5% B. The MRM mass transitions and optimized MS parameters were listed in Figure S1G. The MS transitions and their tuning voltages were selected based on the best response of each precursor/product ion. MS operation conditions were as the following: nebulizing gas, N2, 3 L/minute; drying gas, N2, 15 L/minute; CID gas, Argon 230 psi; interface voltage, 3.5 kV; interface temperature, 300 C; DL temperature, 300 C; heating block temperature, 400°C. Internal calibration method was used for the calculation of concentrations based on 5-point calibration curves. Quantitative analyses were completed using the Shimadzu software LabSolution V. 5.91.

LDH isoenzyme zymography—LDH isoenzyme activities were examined using a native gel electrophoresis method. Briefly, 10–20 mg of mouse tissue was lysed for 10 minutes (10 mM Tris.HCl, 0.1% Triton X-100, 10 mM NaCl, 3 mM $MgCl_2$, pH 7.4). After protein quantification, 30 μg of total proteins per sample were loaded onto a 7.5% non-denaturing polyacrylamide gel (Mini-PROTEAN TG Precast Gels, Bio-Rad) and electrophoresed at 4°C for 2 hours at 200 V. Gel was then placed in the staining solution (10 mL, 0.1 M sodium lactate, 1.5 mM NAD^+, 0.1 M Tris.HCl, 10 mM NaCl, 5 mM $MgCl_2$, pH 8, with 0.3 mg phenazinmethosulphate, 2.5 mg nitrobluetetrazolium) for 10 minutes at 37°C. The gel was then visualized with an Odyssey scanner (model Fc, Li-Cor) and quantified with ImageStudio software (Li-Cor). Protein lysates from mouse muscle and lung were used as positive controls.

Western blotting—Mouse cardiac tissue of 10–20 mg was homogenized using dounce homogenizer in 500 μL RIPA supplemented with protease and phosphate inhibitors (A32959, ThermoFisher) at 4°C. Tissue lysate samples were centrifuged at 14,000 RPM for 15 minutes at 4°C, and protein concentration was measured using a BCA protein assay kit (23225, ThermoFisher). Equal amount (30 μg per lane) of total proteins was loaded onto a Criterion 26-well gel (Bio-Rad). For NRVMs, cells were lysed by adding 1 X SDS-PAGE loading buffer directly to culture plates. After scraping, cell lysates were cleared by passing through glass wool. NRVM proteins were then separated on Criterion 26-well gels and subjected to immunoblotting. Primary antibodies were incubated for overnight, followed by developing with secondary antibodies for 1 hour at room temperature. Immunoblots were visualized with an Odyssey scanner (model Fc, Li-Cor) and quantified with ImageStudio software (Li-Cor).

QUANTIFICATION AND STATISTICAL ANALYSIS

Values are shown as mean ± SEM. Student's t test was used to compare the difference between two groups. One-way ANOVA was conducted for more than 2 groups. For all comparisons with more than 2 variables, two-way ANOVA was performed with subsequent Tukey's test by using GraphPad Prism (V8.0). A $p < 0.05$ was considered statistically significant.

Supplementary Material

Refer to Web version on PubMed Central for supplementary material.

ACKNOWLEDGMENTS

We thank John Shelton and the Molecular Pathology Core of University of Texas Southwestern Medical Center (UTSW) for help with histology. We are grateful to the Animal Resource Center of UTSW for mouse generation, breeding, and maintenance. This work was supported by grants from the American Heart Association (18POST34050049 to G.S.; 14SDG18440002, 17IRG33460191, and 19IPLOI34760325 to Z.V.W.) and NIH (R37-HL034557 to A.D.S.; P41-EB015908 to C.R.M.; R01-DK111430 and R01-CA230631 to J.X.; R01-HL137723 to Z.V.W.).

REFERENCES

Allard MF, Schönekess BO, Henning SL, English DR, and Lopaschuk GD (1994). Contribution of oxidative metabolism and glycolysis to ATP production in hypertrophied hearts. Am. J. Physiol. 267, H742–H750. [PubMed: 8067430]

Benjamin EJ, Muntner P, Alonso A, Bittencourt MS, Callaway CW, Carson AP, Chamberlain AM, Chang AR, Cheng S, Das SR, et al.; American Heart Association Council on Epidemiology and Prevention Statistics Committee and Stroke Statistics Subcommittee (2019). Heart Disease and Stroke Statistics-2019 Update: A Report From the American Heart Association. Circulation 139, e56–e528. [PubMed: 30700139]

Bertero E, and Maack C (2018). Metabolic remodelling in heart failure. Nat. Rev. Cardiol. 15, 457–470. [PubMed: 29915254]

Bi X, Zhang G, Wang X, Nguyen C, May HI, Li X, Al-Hashimi AA, Austin RC, Gillette TG, Fu G, et al. (2018). Endoplasmic Reticulum Chaperone GRP78 Protects Heart From Ischemia/Reperfusion Injury Through Akt Activation. Circ. Res. 122, 1545–1554. [PubMed: 29669712]

Brooks GA (2018). The Science and Translation of Lactate Shuttle Theory. Cell Metab. 27, 757–785. [PubMed: 29617642]

Depre C, Vanoverschelde JL, and Taegtmeyer H (1999). Glucose for the heart. Circulation 99, 578–588. [PubMed: 9927407]

Doenst T, Nguyen TD, and Abel ED (2013). Cardiac metabolism in heart failure: implications beyond ATP production. Circ. Res. 113, 709–724. [PubMed: 23989714]

Doherty JR, and Cleveland JL (2013). Targeting lactate metabolism for cancer therapeutics. J. Clin. Invest. 123, 3685–3692. [PubMed: 23999443]

Drazner MH (2011). The progression of hypertensive heart disease. Circulation 123, 327–334. [PubMed: 21263005]

Faubert B, Li KY, Cai L, Hensley CT, Kim J, Zacharias LG, Yang C, Do QN, Doucette S, Burguete D, et al. (2017). Lactate Metabolism in Human Lung Tumors. Cell 171, 358–371.e9. [PubMed: 28985563]

Favata MF, Horiuchi KY, Manos EJ, Daulerio AJ, Stradley DA, Feeser WS, Van Dyk DE, Pitts WJ, Earl RA, Hobbs F, et al. (1998). Identification of a novel inhibitor of mitogen-activated protein kinase kinase. J. Biol. Chem. 273, 18623–18632. [PubMed: 9660836]

Feng H, Wu J, Chen P, Wang J, Deng Y, Zhu G, Xian J, Huang L, and Ouyang W (2019). MicroRNA-375–3p inhibitor suppresses angiotensin II-induced cardiomyocyte hypertrophy by

promoting lactate dehydrogenase B expression. J. Cell. Physiol. 234, 14198–14209. [PubMed: 30618075]

Gibb AA, and Hill BG (2018). Metabolic Coordination of Physiological and Pathological Cardiac Remodeling. Circ. Res. 123, 107–128. [PubMed: 29929976]

Gladden LB (2004). Lactate metabolism: a new paradigm for the third millennium. J. Physiol. 558, 5–30. [PubMed: 15131240]

Hamada M, Shigematsu Y, Ohtani T, and Ikeda S (2016). Elevated Cardiac Enzymes in Hypertrophic Cardiomyopathy Patients With Heart Failure A 20-Year Prospective Follow-up Study. Circ. J. 80, 218–226. [PubMed: 26549004]

Heineke J, and Molkentin JD (2006). Regulation of cardiac hypertrophy by intracellular signalling pathways. Nat. Rev. Mol. Cell Biol. 7, 589–600. [PubMed: 16936699]

Hill JA, and Olson EN (2008). Cardiac plasticity. N. Engl. J. Med. 358, 1370–1380. [PubMed: 18367740]

Hill JA, Karimi M, Kutschke W, Davisson RL, Zimmerman K, Wang Z, Kerber RE, and Weiss RM (2000). Cardiac hypertrophy is not a required compensatory response to short-term pressure overload. Circulation 101, 2863–2869. [PubMed: 10859294]

Kehat I, and Molkentin JD (2010). Extracellular signal-regulated kinase 1/2 (ERK1/2) signaling in cardiac hypertrophy. Ann. N Y Acad. Sci. 1188, 96–102. [PubMed: 20201891]

Kolwicz SC Jr., Purohit S, and Tian R (2013). Cardiac metabolism and its interactions with contraction, growth, and survival of cardiomyocytes. Circ. Res. 113, 603–616. [PubMed: 23948585]

Kundu BK, Zhong M, Sen S, Davogustto G, Keller SR, and Taegtmeyer H (2015). Remodeling of glucose metabolism precedes pressure overload-induced left ventricular hypertrophy: review of a hypothesis. Cardiology 130, 211–220. [PubMed: 25791172]

Lawrence MC, Jivan A, Shao C, Duan L, Goad D, Zaganjor E, Osborne J, McGlynn K, Stippec S, Earnest S, et al. (2008). The roles of MAPKs in disease. Cell Res. 18, 436–442. [PubMed: 18347614]

Le A, Cooper CR, Gouw AM, Dinavahi R, Maitra A, Deck LM, Royer RE, Vander Jagt DL, Semenza GL, and Dang CV (2010). Inhibition of lactate dehydrogenase A induces oxidative stress and inhibits tumor progression. Proc. Natl. Acad. Sci. USA 107, 2037–2042. [PubMed: 20133848]

Lee DC, Sohn HA, Park ZY, Oh S, Kang YK, Lee KM, Kang M, Jang YJ, Yang SJ, Hong YK, et al. (2015). A lactate-induced response to hypoxia. Cell 161, 595–609. [PubMed: 25892225]

Leong HS, Brownsey RW, Kulpa JE, and Allard MF (2003). Glycolysis and pyruvate oxidation in cardiac hypertrophy–why so unbalanced? Comp. Biochem. Physiol. A Mol. Integr. Physiol. 135, 499–513. [PubMed: 12890541]

Liao R, Jain M, Cui L, D'Agostino J, Aiello F, Luptak I, Ngoy S, Mortensen RM, and Tian R (2002). Cardiac-specific overexpression of GLUT1 prevents the development of heart failure attributable to pressure overload in mice. Circulation 106, 2125–2131. [PubMed: 12379584]

Lopaschuk GD, Spafford MA, and Marsh DR (1991). Glycolysis is predominant source of myocardial ATP production immediately after birth. Am. J. Physiol. 261, H1698–H1705. [PubMed: 1750528]

Lopaschuk GD, Ussher JR, Folmes CD, Jaswal JS, and Stanley WC (2010). Myocardial fatty acid metabolism in health and disease. Physiol. Rev. 90, 207–258. [PubMed: 20086077]

Melotte V, Qu X, Ongenaert M, van Criekinge W, de Bruïne AP, Baldwin HS, and van Engeland M (2010). The N-myc downstream regulated gene (NDRG) family: diverse functions, multiple applications. FASEB J. 24, 4153–4166. [PubMed: 20667976]

Nakamura M, and Sadoshima J (2018). Mechanisms of physiological and pathological cardiac hypertrophy. Nat. Rev. Cardiol. 15, 387–407. [PubMed: 29674714]

Nascimben L, Ingwall JS, Lorell BH, Pinz I, Schultz V, Tornheim K, and Tian R (2004). Mechanisms for increased glycolysis in the hypertrophied rat heart. Hypertension 44, 662–667. [PubMed: 15466668]

Rajman L, Chwalek K, and Sinclair DA (2018). Therapeutic Potential of NAD-Boosting Molecules: The In Vivo Evidence. Cell Metab. 27, 529–547. [PubMed: 29514064]

Readnower RD, Brainard RE, Hill BG, and Jones SP (2012). Standardized bioenergetic profiling of adult mouse cardiomyocytes. Physiol. Genomics 44, 1208–1213. [PubMed: 23092951]

Revis NW, and Cameron AJ (1978). The relationship between fibrosis and lactate dehydrogenase isoenzymes in the experimental hypertrophic heart of rabbits. Cardiovasc. Res. 12, 348–357. [PubMed: 151586]

Ritterhoff J, and Tian R (2017). Metabolism in cardiomyopathy: every substrate matters. Cardiovasc. Res. 113, 411–421. [PubMed: 28395011]

Rogatzki MJ, Ferguson BS, Goodwin ML, and Gladden LB (2015). Lactate is always the end product of glycolysis. Front. Neurosci. 9, 22. [PubMed: 25774123]

Sano M, Minamino T, Toko H, Miyauchi H, Orimo M, Qin Y, Akazawa H, Tateno K, Kayama Y, Harada M, et al. (2007). p53-induced inhibition of Hif-1 causes cardiac dysfunction during pressure overload. Nature 446, 444–448. [PubMed: 17334357]

Sen S, Kundu BK, Wu HC, Hashmi SS, Guthrie P, Locke LW, Roy RJ, Matherne GP, Berr SS, Terwelp M, et al. (2013). Glucose regulation of load-induced mTOR signaling and ER stress in mammalian heart. J. Am. Heart Assoc. 2, e004796. [PubMed: 23686371]

Stanley WC, Recchia FA, and Lopaschuk GD (2005). Myocardial substrate metabolism in the normal and failing heart. Physiol. Rev. 85, 1093–1129. [PubMed: 15987803]

Taegtmeyer H, Sen S, and Vela D (2010). Return to the fetal gene program: a suggested metabolic link to gene expression in the heart. Ann. N Y Acad. Sci. 1188, 191–198. [PubMed: 20201903]

Tran DH, and Wang ZV (2019). Glucose Metabolism in Cardiac Hypertrophy and Heart Failure. J. Am. Heart Assoc. 8, e012673. [PubMed: 31185774]

Tran DH, May HI, Li Q, Luo X, Huang J, Zhang G, Niewold E, Wang X, Gillette TG, Deng Y, and Wang ZV (2020). Chronic activation of hexosamine biosynthesis in the heart triggers pathological cardiac remodeling. Nat. Commun. 11, 1771. [PubMed: 32286306]

Umbarawan Y, Syamsunarno MRAA, Koitabashi N, Yamaguchi A, Hanaoka H, Hishiki T, Nagahata-Naito Y, Obinata H, Sano M, Sunaga H, et al. (2018). Glucose is preferentially utilized for biomass synthesis in pressure-overloaded hearts: evidence from fatty acid-binding protein-4 and -5 knockout mice. Cardiovasc. Res. 114, 1132–1144. [PubMed: 29554241]

Wang YH, Israelsen WJ, Lee D, Yu VWC, Jeanson NT, Clish CB, Cantley LC, Vander Heiden MG, and Scadden DT (2014a). Cell-state-specific metabolic dependency in hematopoiesis and leukemogenesis. Cell 158, 1309–1323. [PubMed: 25215489]

Wang ZV, Deng Y, Gao N, Pedrozo Z, Li DL, Morales CR, Criollo A, Luo X, Tan W, Jiang N, et al. (2014b). Spliced X-box binding protein 1 couples the unfolded protein response to hexosamine biosynthetic pathway. Cell 156, 1179–1192. [PubMed: 24630721]

Wang Y, Zhang Y, Ding G, May HI, Xu J, Gillette TG, Wang H, and Wang ZV (2017). Temporal dynamics of cardiac hypertrophic growth in response to pressure overload. Am. J. Physiol. Heart Circ. Physiol. 313, H1119–H1129. [PubMed: 28822967]

Wang X, Deng Y, Zhang G, Li C, Ding G, May HI, Tran DH, Luo X, Jiang DS, Li DL, et al. (2019). Spliced X-box Binding Protein 1 Stimulates Adaptive Growth Through Activation of mTOR. Circulation 140, 566–579. [PubMed: 31177839]

Xie H, Hanai J, Ren JG, Kats L, Burgess K, Bhargava P, Signoretti S, Billiard J, Duffy KJ, Grant A, et al. (2014). Targeting lactate dehydrogenase–a inhibits tumorigenesis and tumor progression in mouse models of lung cancer and impacts tumor-initiating cells. Cell Metab. 19, 795–809. [PubMed: 24726384]

Yang L, Gao L, Nickel T, Yang J, Zhou J, Gilbertsen A, Geng Z, Johnson C, Young B, Henke C, et al. (2017). Lactate Promotes Synthetic Phenotype in Vascular Smooth Muscle Cells. Circ. Res. 121, 1251–1262. [PubMed: 29021296]

York JW, Penney DG, Weeks TA, and Stagno PA (1976). Lactate dehydrogenase changes following several cardiac hypertrophic stresses. J. Appl. Physiol. 40, 923–926. [PubMed: 132420]

Zhang ZB, Wang CB, Li-Wei, and Qian JQ. (1998). Effects of 1-(2,6-dimethylphenoxy)-2-(3,4-dimethoxyphenylethylamino) propane hydrochloride on heart function, lactate dehydrogenase and its isoenzymes in rats with cardiac hypertrophy. Zhongguo Yao Li Xue Bao 19, 54–57. [PubMed: 10375760]

Zhang D, Contu R, Latronico MV, Zhang J, Rizzi R, Catalucci D, Miyamoto S, Huang K, Ceci M, Gu Y, et al. (2010). MTORC1 regulates cardiac function and myocyte survival through 4E-BP1 inhibition in mice. J. Clin. Invest. 120, 2805–2816. [PubMed: 20644257]

Zhang G, Wang X, Bi X, Li C, Deng Y, Al-Hashimi AA, Luo X, Gillette TG, Austin RC, Wang Y, and Wang ZV (2019). GRP78 (Glucose-Regulated Protein of 78 kDa) Promotes Cardiomyocyte Growth Through Activation of GATA4 (GATA-Binding Protein 4). Hypertension 73, 390–398. [PubMed: 30580686]

Highlights

- Metabolic remodeling plays an important role in hypertensive heart disease
- LDHA as a key enzyme of glycolysis is increased in the hypertrophic heart
- Deficiency of LDHA exacerbates cardiomyopathy under pressure overload
- LDHA may be required for adaptive hypertrophic growth via NDRG3 stimulation

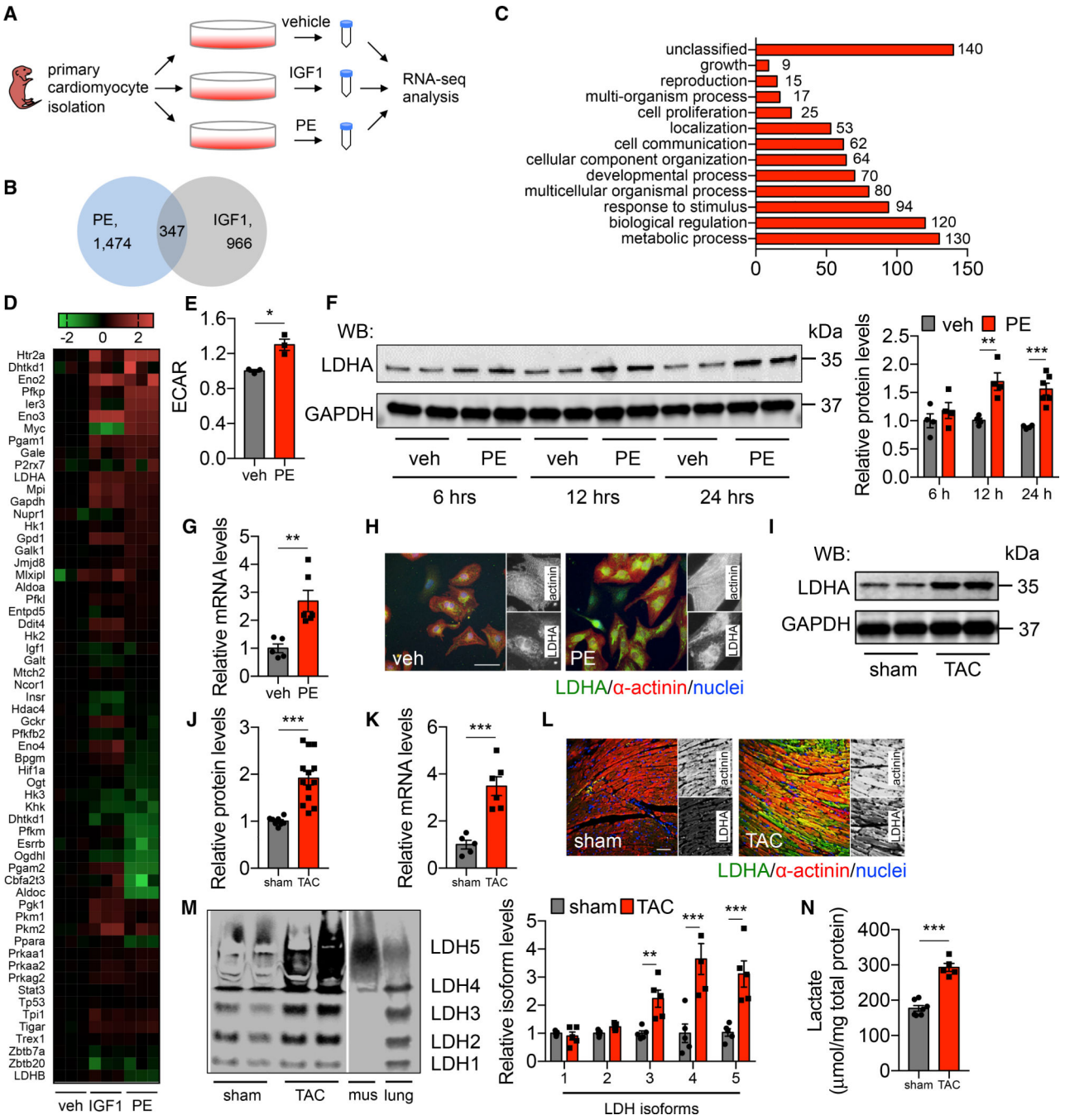

Figure 1. LDHA Is Induced in the Heart by Hypertrophic Growth

(A) Schematic representation of RNA-seq analysis. Neonatal rat ventricular myocytes (NRVMs) were isolated from 1–2-day-old Sprague-Dawley rats and treated by either insulin-like growth factor 1 (IGF1) or phenylephrine (PE). Total RNA was isolated for RNA-seq analysis. n = 3 for each group.

(B) Venn diagram showing the numbers of genes enriched in PE and IGF1 treatments (cutoff > 1.4, $p < 0.01$).

(C) The commonly changed genes between PE and IGF1 treatments (n = 347) were subjected to IPA (ingenuity pathway analysis). Note that metabolic process ranks the first, with the most altered genes.

(D) Heatmap showing the expression of genes involved in glucose utilization pathways, analyzed from RNA-seq data.

(E) PE treatment increased glycolytic rate of NRVMs as measured by extracellular acidification rate analysis (ECAR). n = 3.

(F) PE treatment in NRVMs led to a significant increase in LDHA expression at the protein level (quantified at right). n = 4–6.

(G) The mRNA level of LDHA was elevated by PE treatment. n = 5–6.

(H) Immunofluorescent staining showed the increase of LDHA in cardiomyocytes after PE treatment. α-Actinin was used as a cardiomyocyte marker. Scale bar, 100 μm.

(I) LDHA protein expression was increased by pressure overload in the heart. Thoracic aortic constriction (TAC) was conducted for 7 days in wild-type C57BL/6 mice. Sham operation was similarly done but without constriction. Cardiac tissues were used for western blotting.

(J) Quantification of (I) showed a significant increase of LDHA by pressure overload in the heart. n = 8–13.

(K) The mRNA level of LDHA was elevated by TAC in the heart. n = 5–6.

(L) Expression and localization of LDHA was visualized by immunostaining in mouse left ventricular tissues at day 7 after TAC. α-Actinin was used as a cardiomyocyte marker. Scale bar, 50 μm.

(M) In-gel enzymatic assay showed activities of various LDH isoenzymes from mouse left ventricular tissues at day 7 after TAC. Mouse skeletal muscle (mainly LDHA isoform) and lung (all isoforms) tissues were used as controls. n = 5.

(N) Cardiac tissue lactate content was increased by TAC as determined by LC/MS/MS. n = 5–7.

Data are represented as mean ± SEM. Student’s t test was conducted. *$p < 0.05$; **$p < 0.01$; ***$p < 0.001$. See also Figure S1.

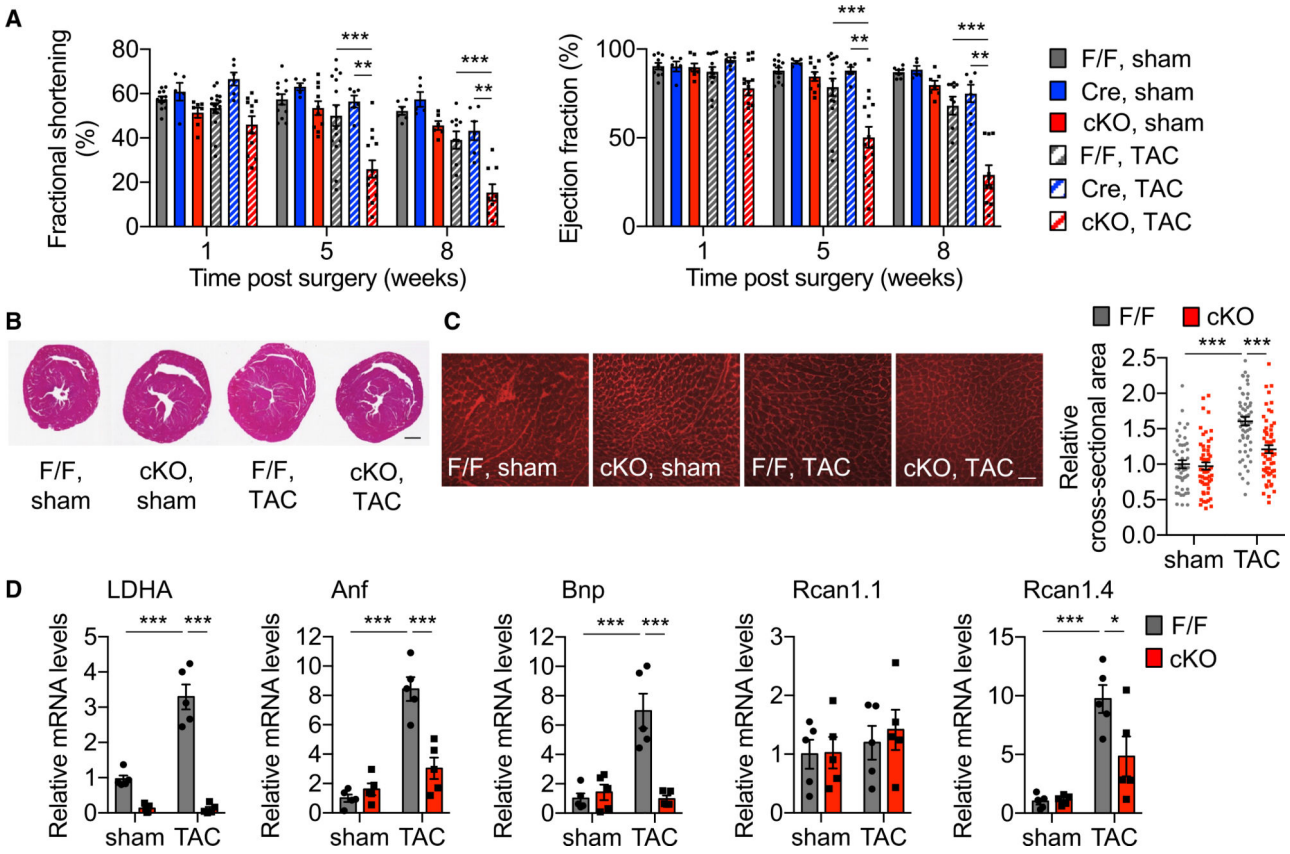

Figure 2. LDHA Is Required for Cardiac Hypertrophic Growth in Response to Pressure Overload *In Vivo*

(A) Cardiac systolic function was impaired in the cardiomyocyte-specific LDHA conditional knockout (cKO) mice compared with either αMHC-Cre or $LDHA^{F/F}$ (F/ F) controls after TAC, as examined by echocardiography. n = 5–15.

(B) Hematoxylin and eosin (H&E) staining showed less cardiac growth of the cKO mice after TAC. Scale bar, 1 mm.

(C) Cardiac tissue sections were used for wheat germ agglutinin (WGA) staining to visualize cardiac cells (left). Scale bar, 100 μm. Quantification of cardiomyocyte cross-sectional area is shown at right. A significance decrease was found in cKO mice after TAC compared to controls. A total of 46–59 cardiomyocytes were quantified for each group. n = 4 mice per group.

(D) Molecular markers of cardiac hypertrophic growth were significantly induced by TAC in control mice, while deficiency of LDHA inhibited the elevation. Rcan1.1 was used as a negative control. n = 5.

Data are represented as mean ± SEM. Two-way ANOVA, followed by Tukey's test, was used to determine statistical differences. *p < 0.05; **p < 0.01; ***p < 0.001. See also Figures S2 and S3.

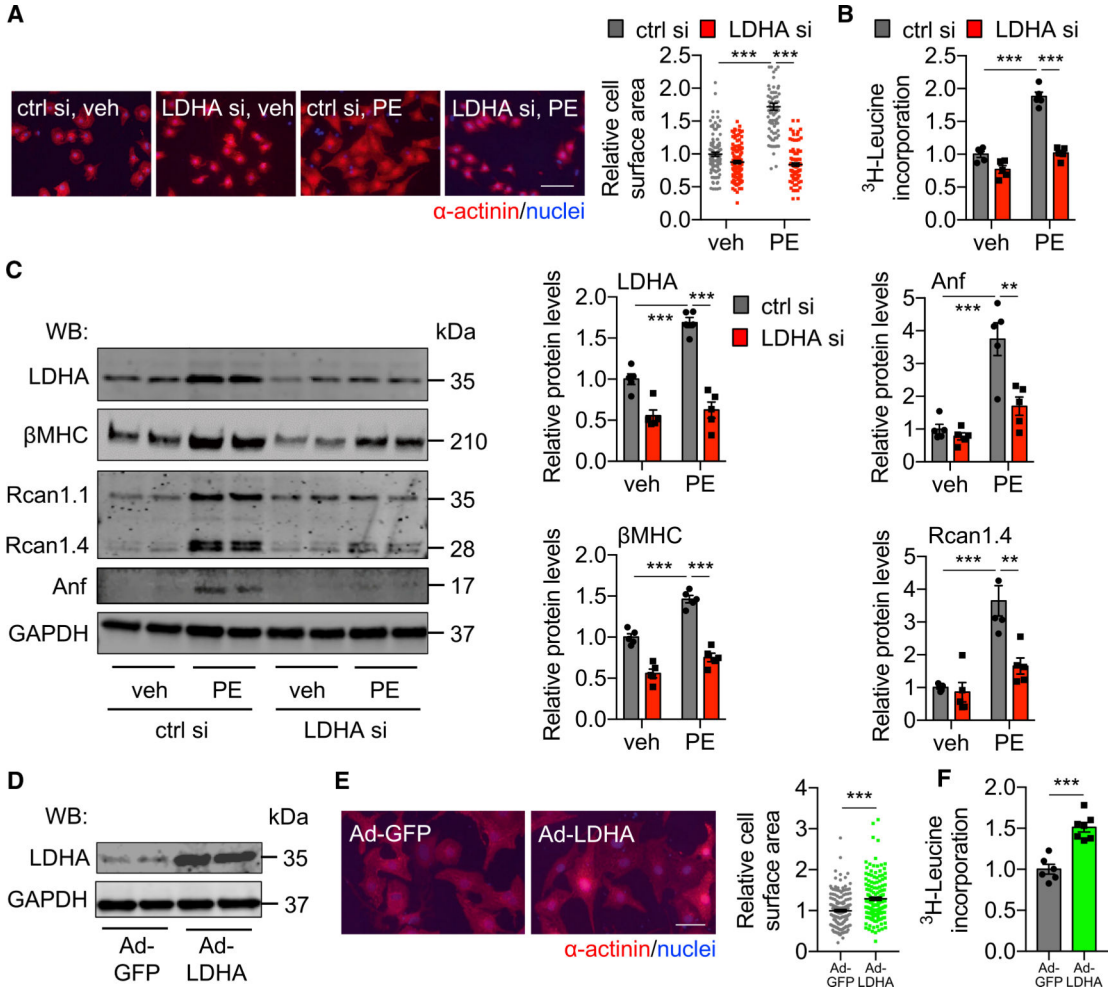

Figure 3. LDHA Is Necessary and Sufficient to Drive Cardiomyocyte Growth

(A) PE treatment led to an increase in cell size of NRVMs, which was strongly inhibited by LDHA silencing. Scale bar, 100 μm. Quantification is shown at right. A total of 91–118 cardiomyocytes were quantified for individual groups.

(B) LDHA knockdown reduced protein synthesis from PE treatment, as assessed by radioactive leucine incorporation. n = 5.

(C) Protein expression of hypertrophic growth markers was decreased by LDHA silencing in NRVMs. Quantification is shown at right. n = 5.

(D) Overexpression of LDHA in NRVMs by adenovirus infection.

(E) Overexpression of LDHA in NRVMs led to a significant increase in cardiomyocyte size. Scale bar, 50 μm. n = 151–177 cardiomyocytes from each group.

(F) LDHA overexpression was sufficient to increase protein synthesis in NRVMs, as determined by radioactive leucine incorporation. n = 6–7.

Data are represented as mean ± SEM. Two-way ANOVA, followed by Tukey's test, was used to determine statistical differences for (A)–(C). Student's t test was conducted for (E) and (F). **p < 0.01; ***p < 0.001. See also Figure S4.

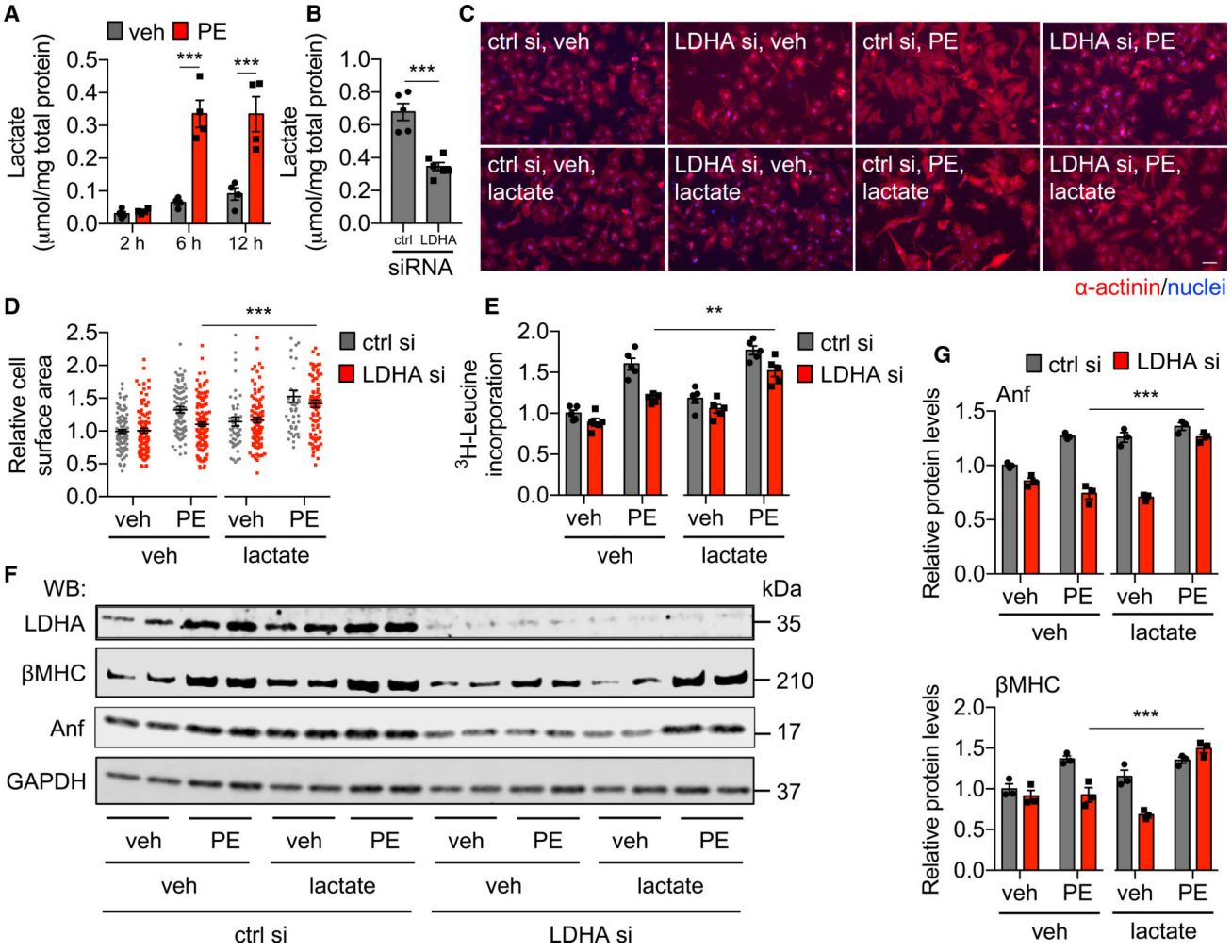

Figure 4. LDHA-Derived Lactate Potentiates Cardiomyocyte Hypertrophic Growth

(A) PE treatment in NRVMs increased cellular lactate level as determined by the LC/MS/MS approach. Lactate level was normalized to total protein content. n = 4.

(B) LDHA silencing by siRNA led to a significant decrease in cellular lactate level. n = 5–6.

(C) Lactate treatment rescued the cell growth defect from LDHA knockdown. NRVMs were first transfected with negative control or LDHA siRNA oligos. PE (50 μM) treatment was conducted in the presence of vehicle or lactate (20 mM). Scale bar, 50 μm.

(D) Quantification showed lactate treatment rescued cell growth from LDHA silencing. n = 46–132 cardiomyocytes for each group.

(E) Lactate treatment in NRVMs rescued protein synthesis from LDHA silencing, as assessed by ^{3}H-leucine incorporation assay. n = 5.

(F) Protein expression of hypertrophic markers was examined by immunoblotting.

(G) Lactate supplementation led to a significant increase in protein levels of hypertrophic markers, quantified from (F). n = 3.

Data are represented as mean ± SEM. Student's t test was conducted for (A) and (B). Two-way ANOVA was conducted, followed by Tukey's test, to determine statistical differences for (D), (E), and (G). **p < 0.01; ***p < 0.001. See also Figure S5.

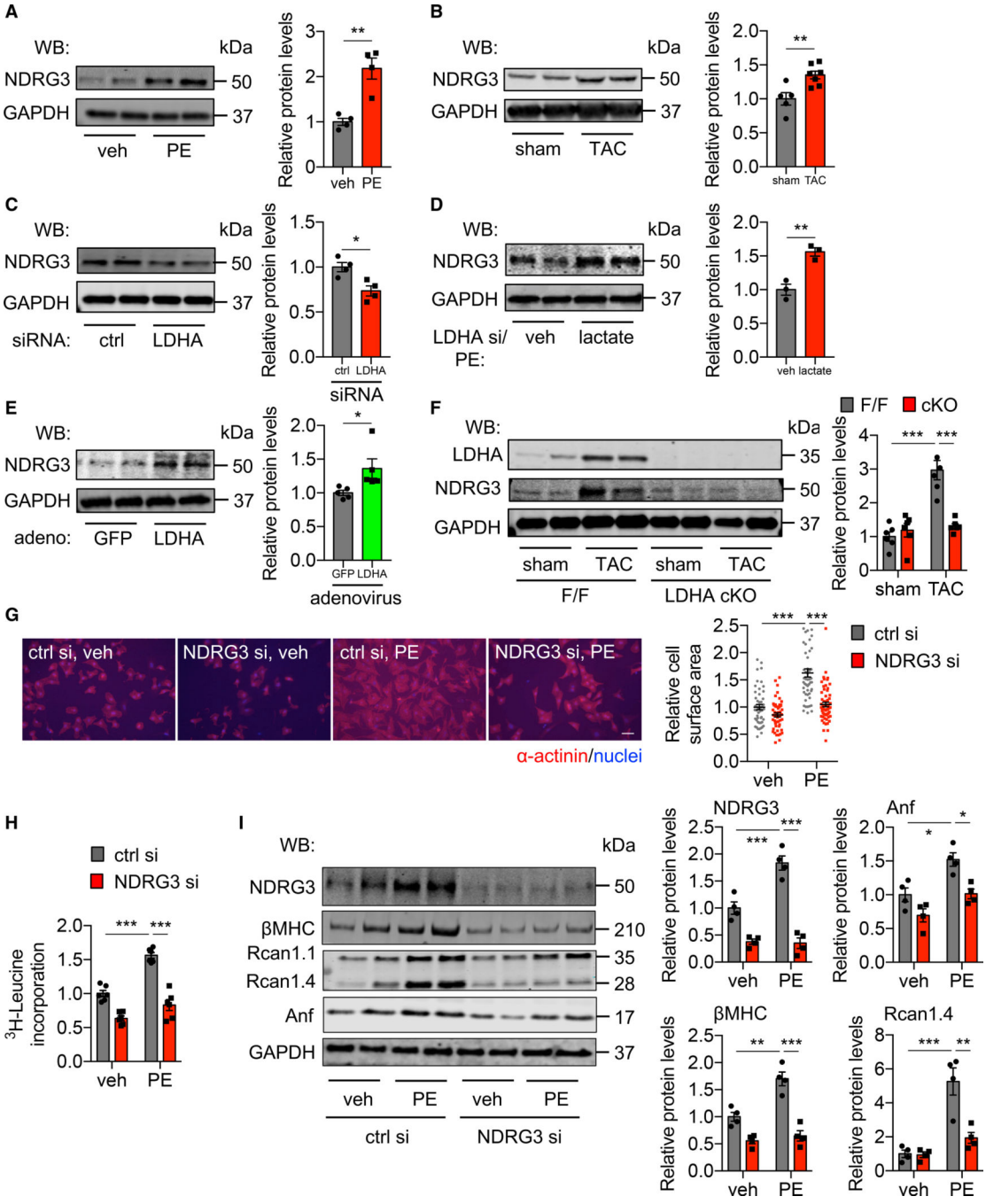

Figure 5. NDRG3 Expression Is Upregulated by LDHA

(A) Cardiomyocyte hypertrophic growth induced by PE led to an increase in NDRG3 protein expression. NRVMs were treated with PE (50 μM) for 24 h. n = 4.

(B) NDRG3 was increased in the heart by TAC. Mouse cardiac tissues were used for western blotting at 1 week after TAC. n = 5–7.

(C) LDHA silencing in NRVMs decreased NDRG3 expression. n = 4.

(D) Lactate treatment rescued NDRG3 protein expression from LDHA silencing. n = 3.

(E) Overexpression of LDHA in NRVMs caused an increase in NDRG3. n = 5.

(F) NDRG3 expression was reduced in the heart by LDHA deficiency. Control and LDHA cKO mice were subjected to TAC for 1 week. Cardiac tissues were harvested for immunoblotting. n = 6.

(G) NDRG3 silencing led to a decrease in cardiomyocyte growth after PE treatment. Scale bar, 50 μm. n = 50–61 cells for each group.

(H) Knockdown of NDRG3 decreased protein synthesis as examined by ^{3}H-leucine incorporation in NRVMs. n = 6.

(I) NDRG3 silencing led to a decrease in protein expression of hypertrophic markers in NRVMs. n = 4.

Data are represented as mean ± SEM. Student's t test was conducted for (A)–(E). Two-way ANOVA was conducted, followed by Tukey's test, to determine statistical differences for (F)–(I). *p < 0.05; **p < 0.01; ***p < 0.001. See also Figures S5 and S6.

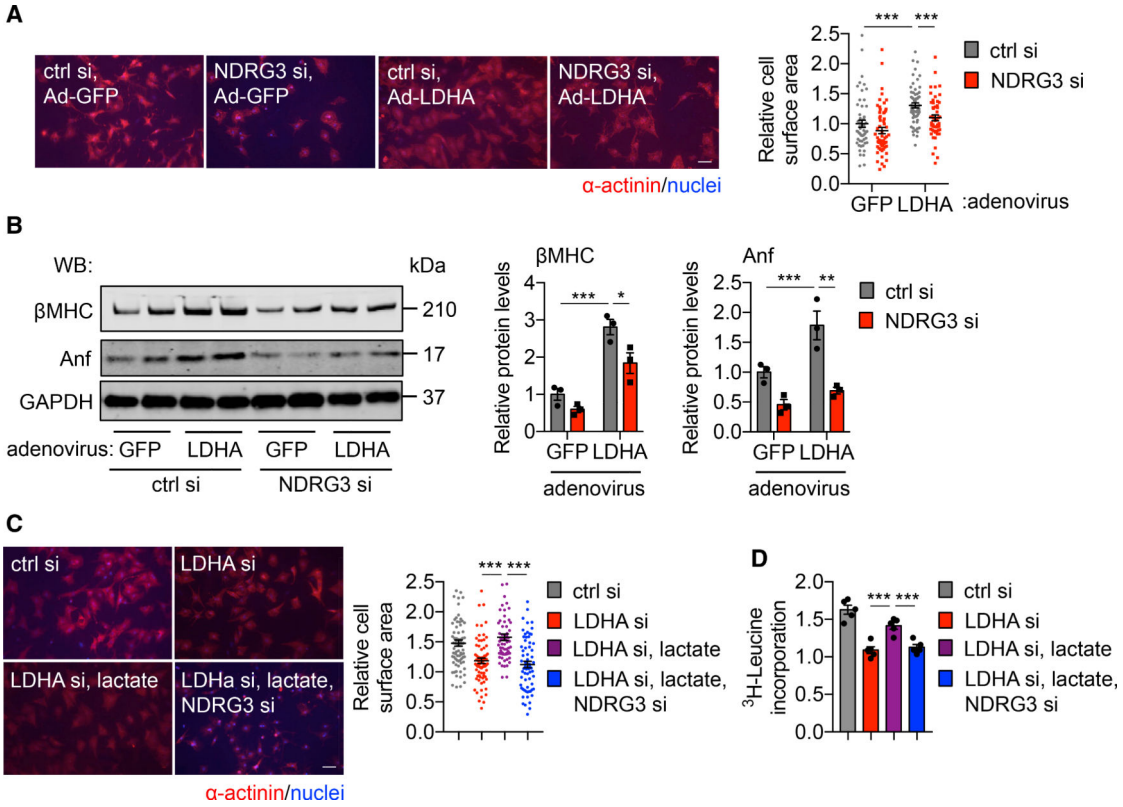

Figure 6. NDRG3 Is Required for LDHA-Mediated Hypertrophic Growth

(A) Knockdown of NDRN3 led to a decrease of cardiomyocyte growth. NRVMs were infected by adenovirus expressing either control GFP or LDHA. Control or NDRG3 siRNA oligo was then used to transfect the cells. Scale bar, 50 μm. n = 52–63 cardiomyocytes for individual groups.

(B) Silencing of NDRG3 reduced protein expression of hypertrophic markers. n = 3.

(C) The rescue effect from lactate supplementation on cardiomyocyte size was eliminated by NDRG3 silencing. Scale bar, 50 μm. n = 65–72 cells for each group.

(D) NDRG3 knockdown inhibited the lactate effect on protein synthesis as revealed by ^{3}H-leucine incorporation. n = 5.

Data are represented as mean ± SEM. Two-way ANOVA was conducted, followed by Tukey's test, to determine statistical differences. *p < 0.05; **p < 0.01; ***p < 0.001. See also Figure S6.

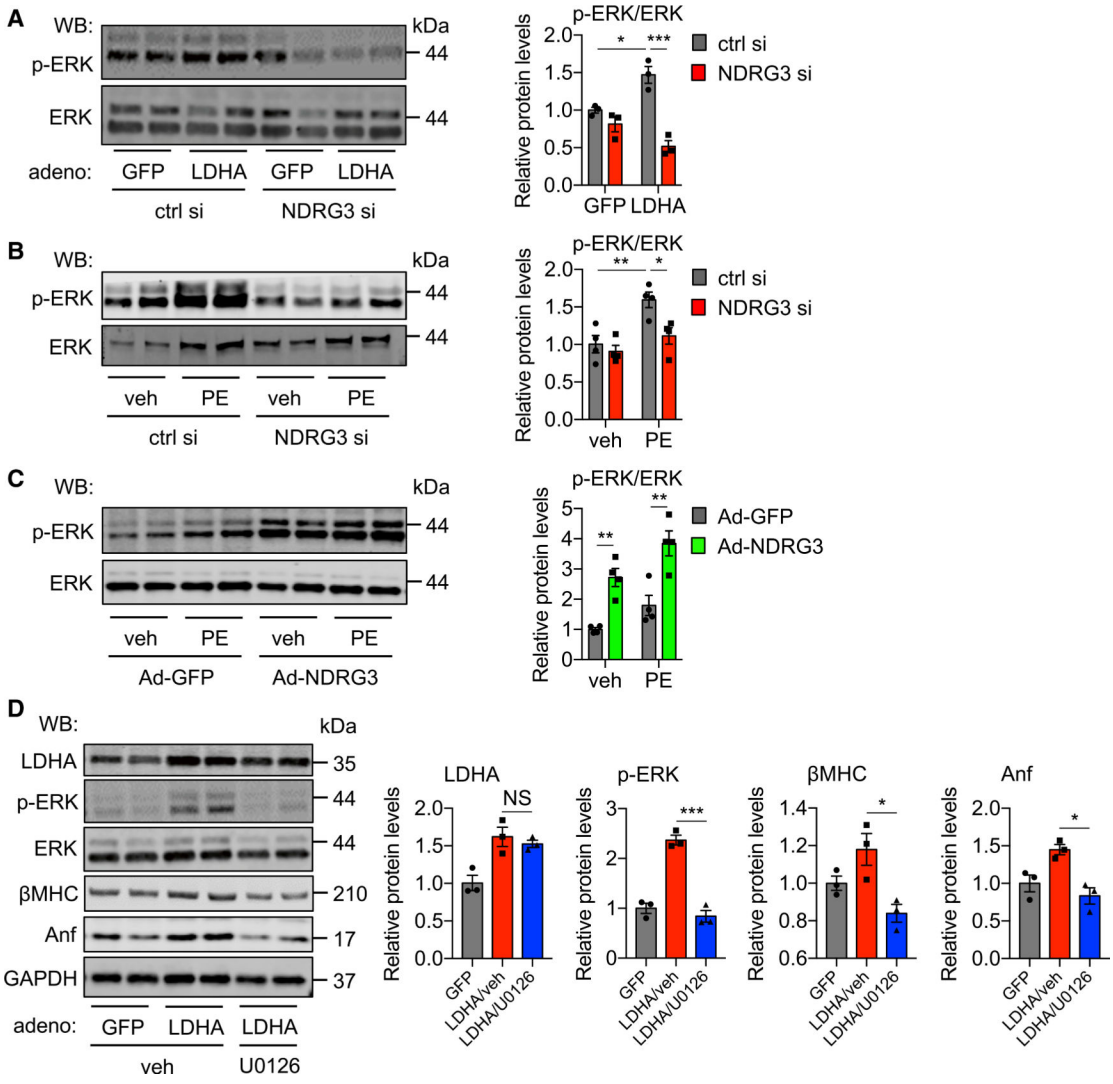

Figure 7. The LDHA/NDRG3 Axis Activates ERK in Cardiac Hypertrophic Growth

(A) NDRG3 knockdown decreased ERK signaling from LDHA overexpression in NRVMs. n = 3.

(B) NDRG3 silencing inhibited ERK phosphorylation from PE treatment. n = 4.

(C) Overexpression of NDRG3 potentiated PE-induced ERK activation. n = 4.

(D) Inhibition of ERK signaling led to suppression of cardiomyocyte growth from LDHA overexpression. n = 3.

Data are represented as mean ± SEM. Two-way ANOVA was conducted, followed by Tukey's test, to determine statistical differences for (A)–(C). Student's t test was conducted for (D). NS, not significant; *p < 0.05; **p < 0.01; ***p < 0.001. See also Figure S7.

KEY RESOURCES TABLE

REAGENT or RESOURCE	SOURCE	IDENTIFIER
Antibodies		
Rabbit polyclonal anti-LDHA	Cell Signaling Technology	Cat# 2012; RRID:AB_2137173
Rabbit polyclonal anti-NDRG3	Cell Signaling Technology	Cat#5846; RRID:AB_10705524
Rabbit monoclonal anti-p44/42 MAPK (ERK1/2)	Cell Signaling Technology	Cat#4695; RRID:AB_390779
Rabbit monoclonal anti-phospho-p44/42 MAPK (ERK1/2)	Cell Signaling Technology	Cat#4370; RRID:AB_2315112
Mouse monoclonal anti-GAPDH	Fitzgerald	Cat#10R-G109a; RRID:AB_1285808
Rabbit polyclonal anti-DSCR1 (Rcan1)	Sigma	Cat#D6694; RRID:AB_2179743
Rabbit polyclonal anti-Natriuretic peptides A (Anf)	Abcam	Cat#ab180649; RRID:AB_2858196
Mouse monoclonal anti-Raf-1 (C-10)	Santa Cruz Biotechnology	Cat#sc-373722; RRID:AB_10947103
Mouse monoclonal anti-Heavy chain cardiac myosin	Abcam	Cat#ab50967; RRID:AB_942084
Mouse monoclonal anti-p-Raf1 (E-1)	Santa Cruz Biotechnology	Cat#sc-271929; RRID: AB_10659238
Mouse monoclonal anti-alpha-Actinin	Sigma	Cat#A7811; RRID:AB_476766
Goat anti-Rabbit IgG IRDye 800CW	LI-COR	Cat#925–32211; RRID: AB_2651127
Goat anti-Mouse IgG Alexa Fluor 700	ThermoFisher Scientific	Cat#A-21036; RRID:AB_2535707
Rabbit polyclonal anti-HMGB1	Cell Signaling Technology	Cat#3935; RRID:AB_2295241
Rabbit polyclonal anti-Caspase 3	Cell Signaling Technology	Cat#9662; RRID:AB_331439
Rabbit polyclonal anti-cleaved Caspase 3	Cell Signaling Technology	Cat#9661; RRID:AB_2341189
Rabbit polyclonal anti-Caspase 12	Cell Signaling Technology	Cat#2202; RRID:AB_2069200
Bacterial and Virus Strains		
Adenovirus LDHA overexpression	This study	N/A
Adenovirus NDRG3 overexpression	This study	N/A
Deposited Data		
RNA-seq data	This study	GSE153763
Experimental Models: Organisms/Strains		
Mouse αMHC-Cre	This study	N/A
Mouse $LDHA^{F/F}$	Wang et al., 2014a	N/A
Oligonucleotides		
Rat NDRG3 siRNA #1	Sigma	Cat#SASI_Rn02_00201215
Rat NDRG3 siRNA #2	Sigma	Cat#SASI_Rn02_00201214
Rat LDHA siRNA #1	Sigma	Cat#SASI_Rn01_0046924
Rat LDHA siRNA #2	Sigma	Cat#SASI_Rn01_0046925
Primers for RT-PCR and genotyping, see Table S1.	Sigma	N/A